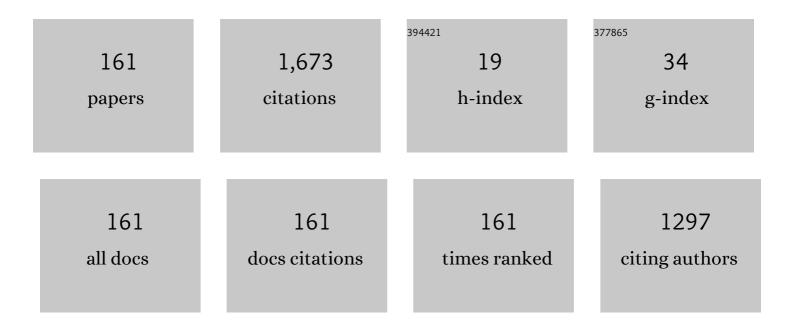
## Dmitriy Yu Kovalev

List of Publications by Year in descending order

Source: https://exaly.com/author-pdf/6360391/publications.pdf Version: 2024-02-01



#	Article	IF	CITATIONS
1	Fast mechanical synthesis, structure evolution, and thermal stability of nanostructured CoCrFeNiCu high entropy alloy. Journal of Alloys and Compounds, 2022, 893, 161839.	5.5	16
2	Thermal expansion of the nanocrystalline titanium diboride. Ceramics International, 2022, 48, 872-878.	4.8	5
3	Engineering of strong and hard in-situ Al-Al3Ti nanocomposite via high-energy ball milling and spark plasma sintering. Journal of Alloys and Compounds, 2022, 895, 162676.	5.5	10
4	<i>In situ</i> study of heterogeneous media combustion processes by time Resolved XRD. Zavodskaya Laboratoriya Diagnostika Materialov, 2022, 88, 49-61.	0.5	0
5	Mechanical alloying in the Co-Fe-Ni powder mixture: Experimental study and molecular dynamics simulation. Powder Technology, 2022, 399, 117187.	4.2	8
6	Effects of titanium high energy ball milling on the solid-phase reaction Ti+C. Materials Chemistry and Physics, 2022, 283, 126025.	4.0	6
7	Investigation of the Structure of Cyclodextrin Nitrates by the X-Ray Diffraction Method. Russian Journal of Applied Chemistry, 2022, 95, 32-36.	0.5	0
8	Combustion Modes of Mixtures of Nickel (II) Oxide with Titanium. Fizika Goreniya I Vzryva, 2021, 57, 69-72.	0.0	0
9	Subtle Details in Crystal Structure of SHS Products by DFT Calculations. International Journal of Self-Propagating High-Temperature Synthesis, 2021, 30, 15-21.	0.5	0
10	Evolution of crystal structure in high-entropy AlCoCrFeNi alloy: An in situ high-temperature X-ray diffraction study. Journal of Alloys and Compounds, 2021, 861, 158562.	5.5	15
11	SHS in the Si–N–O System Containing Iron Salts. International Journal of Self-Propagating High-Temperature Synthesis, 2021, 30, 65-72.	0.5	Ο
12	The Concentration of C(sp3) Atoms and Properties of an Activated Carbon with over 3000 m2/g BET Surface Area. Nanomaterials, 2021, 11, 1324.	4.1	11
13	Synthesis of W–Zr–Ti Alloy via Combustion in the WO3–ZrO2–TiO2–Mg System. Inorganic Materials, 2021, 57, 498-502.	0.8	0
14	Thermal Stability of Medium- and High-Entropy Alloys of 3d-Transition Metals. Journal of Phase Equilibria and Diffusion, 2021, 42, 720-734.	1.4	7
15	SHS in the Cu–Se System. International Journal of Self-Propagating High-Temperature Synthesis, 2021, 30, 180-184.	0.5	1
16	Fabrication of high-entropy carbide (TiZrHfTaNb)Ðį by high-energy ball milling. Ceramics International, 2021, 47, 32626-32633.	4.8	20
17	Comprehensive Study on the Mechanism of Sulfating Roasting of Zinc Plant Residue with Iron Sulfates. Materials, 2021, 14, 5020.	2.9	7
18	Reduction of Mn, Cr, and V Precursors in a Wave of Flameless RDX Combustion. International Journal of Self-Propagating High-Temperature Synthesis, 2021, 30, 11-14.	0.5	1

#	Article	IF	CITATIONS
19	Combustion Modes of Mixtures of Copper (II) Oxide with Aluminum and Titanium. Fizika Goreniya I Vzryva, 2021, 57, 67-73.	0.0	Ο
20	Combustion Modes of Mixtures of Copper (II) Oxide with Aluminum and Titanium. Combustion, Explosion and Shock Waves, 2021, 57, 570-575.	0.8	0
21	Synthesis and Thermal Oxidation Stability of Nanocrystalline Niobium Diboride. Inorganic Materials, 2021, 57, 1005-1014.	0.8	4
22	Synthesis of Cu2 – nSe via Autowave Combustion of an Elemental Powder Mixture. Inorganic Materials, 2021, 57, 1124-1134.	0.8	1
23	Synthesis of Nanosized FeS, CoS and NiS Crystals in a Wave of Flameless RDX Combustion. International Journal of Self-Propagating High-Temperature Synthesis, 2021, 30, 220-224.	0.5	1
24	The Synthesis of Cast Materials Based on the MAX Phases in a Cr–Ti–Al–C System. Russian Journal of Non-Ferrous Metals, 2021, 62, 732-739.	0.6	1
25	Obtaining a High-Entropy Fe–Cr–Co–Ni–Ti Alloy by Mechanical Alloying and Electric Spark Plasma Sintering of a Powder Mixture. Russian Journal of Non-Ferrous Metals, 2021, 62, 716-722.	0.6	0
26	High-Temperature Synthesis of Cr–Mo–Al–C Materials. Inorganic Materials, 2021, 57, 1300-1306.	0.8	2
27	Synthesis of Ta4HfC5 Ceramics with a Submicron Structure by Electro-Thermal Explosion under Pressure. Doklady Chemistry, 2021, 501, 259-263.	0.9	1
28	The Influence of Molybdenum and Titanium on Magnetic and Mechanical Properties of Fe–30Cr–16Co (Kh30K16) Powder Hard Magnetic Alloy. Steel in Translation, 2021, 51, 939-944.	0.3	0
29	Structural evolution and magnetic properties of high-entropy CuCrFeTiNi alloys prepared by high-energy ball milling and spark plasma sintering. Journal of Alloys and Compounds, 2020, 816, 152611.	5.5	29
30	Combustion synthesis of TiC-based ceramic-metal composites with high entropy alloy binder. Journal of the European Ceramic Society, 2020, 40, 2527-2532.	5.7	35
31	Synthesis, Structure and Properties of Material Based on V2AIC MAX Phase. Physics of Metals and Metallography, 2020, 121, 765-771.	1.0	13
32	Composition and Crystalline Structure of Ternary Phases in the Ta–Ni–Al System. Russian Journal of Non-Ferrous Metals, 2020, 61, 303-308.	0.6	1
33	Synthesis, Structure, and Properties of Titanium Diboride Nanoparticles. Inorganic Materials, 2020, 56, 1127-1132.	0.8	2
34	X-Ray Diffraction Analysis of the Amorphous–Crystalline Phase Transition in Ni. Technical Physics, 2020, 65, 1652-1658.	0.7	0
35	Assembling the Puzzle of Taxifolin Polymorphism. Molecules, 2020, 25, 5437.	3.8	12
36	Mo5SiB2-Based Ceramics by Forced SHS Compaction and Hot Pressing of SHS-Produced Powders: Features of Phase-Formation Processes. International Journal of Self-Propagating High-Temperature Synthesis, 2020, 29, 143-149.	0.5	1

#	Article	IF	CITATIONS
37	High-Energy Ball Milling and Spark Plasma Sintering of the CoCrFeNiAl High-Entropy Alloy. Metals, 2020, 10, 1489.	2.3	11
38	Structure and properties of MoSi2–MeB2–SiC (Me = Zr, Hf) ceramics produced by combination of SHS and HP techniques. Ceramics International, 2020, 46, 28725-28734.	4.8	16
39	High temperature X-ray powder diffraction study of boron carbide crystals of different composition. Journal of Solid State Chemistry, 2020, 290, 121579.	2.9	2
40	Density Functional Theory Calculations of the Stability and Statistical Disorder in Crystals of the Kappa Phase of Me3Â+ÂxW10–ÂxC3Â+Ây (Me = Fe, Co, Ni). Russian Journal of Physical Chemistry A, 2020, 94, 1369-1374.	, 0.6	0
41	Synthesis of the Ti3SiC2 MAX Phase via Combustion in the TiO2–Mg–Si–C System. Inorganic Materials, 2020, 56, 1211-1216.	0.8	2
42	X-Ray Diffraction Study of a New Phase in the Ni–W–C System. Inorganic Materials, 2020, 56, 572-576.	0.8	1
43	Preparation of Ti2AlC and Ti3AlC2 MAX Phases by Self-Propagating High-Temperature Synthesis with the Reduction Stage. Russian Journal of Non-Ferrous Metals, 2020, 61, 554-558.	0.6	2
44	Ti–W Composite by Magnesiothermic SHS and Acid Leaching. International Journal of Self-Propagating High-Temperature Synthesis, 2020, 29, 36-41.	0.5	0
45	DFT – Driven design of hierarchically structured, strong and highly conductive alloys in Cu–Ti system via in situ hydration - re-oxidation. Journal of Alloys and Compounds, 2020, 832, 154823.	5.5	2
46	Synthesis of Titanium Diboride Nanoparticles via the Reaction of TiCl4 with NaBH4 in NaCl‒KCl Ionic Melt. Russian Journal of General Chemistry, 2020, 90, 924-926.	0.8	2
47	One-step synthesis of pure γ-FeNi alloy by reaÑŧive sol–gel combustion route: mechanism and properties. Journal of Sol-Gel Science and Technology, 2020, 94, 310-321.	2.4	18
48	Formation of New Intermetallic Phases in the Ta–Ni–Al System. Inorganic Materials: Applied Research, 2020, 11, 271-276.	0.5	0
49	Synthesis of Vanadium Diboride Nanoparticles via Reaction of VCl3 with NaBH4. Inorganic Materials, 2020, 56, 126-131.	0.8	4
50	Thermal Expansion of Micro- and Nanocrystalline ZrB2 Powders. Inorganic Materials, 2020, 56, 258-264.	0.8	3
51	Self-Propagating High-Temperature Synthesis of MgAl2O4 Spinel. Inorganic Materials, 2020, 56, 142-150.	0.8	9
52	Synthesis of Nb2AlC MAX Phase by SHS Metallurgy. Russian Journal of Non-Ferrous Metals, 2020, 61, 126-131.	0.6	7
53	Spall Strength of Shock-Heated Zirconium and Phase Diagram of Its High-Pressure Polymorphic Modification. Physics of the Solid State, 2020, 62, 65-73.	0.6	2
54	Single crystals of ferroelectric lithium niobate–tantalate LiNb <sub>1–<i>x</i> </sub> Ta <i> <sub> <i>x</i> </sub> </i> O <sub>3</sub> solid solutions for high-temperature sensor and actuator applications. Acta Crystallographica Section B: Structural Science, Crystal Engineering and Materials, 2020, 76, 1071-1076.	1.1	17

#	Article	IF	CITATIONS
55	Estimation of Enthalpy of Formation of TiCu by Density Functional Method. Physics of Metals and Metallography, 2020, 121, 1188-1192.	1.0	4
56	Obtaining of Ti <sub>2</sub> AlC and Ti <sub>3</sub> AlC <sub>2</sub> MAX phases by SHS with reduction stage. Izvestiya Vuzov Poroshkovaya Metallurgiya I Funktsional'nye Pokrytiya, 2020, , 36-40.	0.2	0
57	Phase Formation in the SHS of a Ti–B Mixture with the Addition of Si3N4. Combustion, Explosion and Shock Waves, 2020, 56, 648-654.	0.8	9
58	Cu-Matrix Composites by Reactive Spark Plasma Sintering of Mechanoactivated Cu–Si–C Powder Mixtures. International Journal of Self-Propagating High-Temperature Synthesis, 2020, 29, 233-236.	0.5	2
59	Thermal Expansion of Micro- and Nanocrystalline HfB2. High Temperature, 2019, 57, 32-36.	1.0	9
60	Processing of Ni–Al intermetallic with 2D carbon components. Materials Chemistry and Physics, 2019, 238, 121898.	4.0	7
61	Structure and properties of equiatomic CoCrFeNiMn alloy fabricated by high-energy ball milling and spark plasma sintering. Journal of Alloys and Compounds, 2019, 805, 1237-1245.	5.5	41
62	Time-Resolved X-Ray Diffraction in SHS Research and Related Areas: An Overview. International Journal of Self-Propagating High-Temperature Synthesis, 2019, 28, 114-123.	0.5	13
63	Estimating the Stability of the Structure of MAX Phases of Ti3AlC2–ÂÑBÑ Composition on the Basis of Quantum-Chemical Calculations. Russian Journal of Physical Chemistry A, 2019, 93, 1277-1280.	0.6	1
64	Phase Formation in the Ti–Al–C System during SHS. Russian Journal of Non-Ferrous Metals, 2019, 60, 61-67.	0.6	8
65	TiZrNiCuAl and TiNbNiCuAl Alloys by Thermal Explosion and High-Energy Ball Milling. International Journal of Self-Propagating High-Temperature Synthesis, 2019, 28, 137-142.	0.5	2
66	Ti–Zr Alloy by Magnesiothermic Reduction and Acid Leaching: Influence of Process Conditions. International Journal of Self-Propagating High-Temperature Synthesis, 2019, 28, 187-190.	0.5	1
67	Feasibility of Producing a Ti–Zr Alloy via Combustion in the TiO2–ZrO2–Mg System. Inorganic Materials, 2019, 55, 185-190.	0.8	3
68	Preparation of ZrB2 by Reacting ZrCl4 with NaBH4 in Molten Potassium Bromide. Inorganic Materials, 2019, 55, 458-461.	0.8	2
69	Influence of the Preparation Method on Amorphous-Crystalline Transition in Fe84B16 Alloy. Technical Physics, 2019, 64, 1808-1813.	0.7	1
70	High-Temperature X-ray Diffraction Study of the Thermal Expansion and Stability of Nanocrystalline VB2. Inorganic Materials, 2019, 55, 1111-1117.	0.8	4
71	Boron Carbide Secrets. Russian Journal of General Chemistry, 2019, 89, 2069-2074.	0.8	2
72	Direct Conversion of Chemical Energy into Electrical Energy in the Combustion of a Thin Three-Layer Charge. Combustion, Explosion and Shock Waves, 2019, 55, 678-685.	0.8	1

#	Article	IF	CITATIONS
73	Self-propagating high-temperature synthesis of advanced ceramics MoSi2–HfB2–MoB. Ceramics International, 2019, 45, 96-107.	4.8	43
74	High-temperature synthesis of cast materials based on Nb2AlC MAX phase. Ceramics International, 2019, 45, 2689-2691.	4.8	14
75	Combustion synthesis of ZrB2-TaB2-TaSi2 ceramics with microgradient grain structure and improved mechanical properties. Ceramics International, 2019, 45, 1503-1512.	4.8	22
76	Nb2AlC MAX phase synthesis by SHS metallurgy. Izvestiya Vuzov Poroshkovaya Metallurgiya I Funktsional'nye Pokrytiya, 2019, , 42-48.	0.2	2
77	Formation of new intermetallic phases in the Ta – Ni – Al system. Perspektivnye Materialy, 2019, , 5-13.	0.1	3
78	Mechanochemical Synthesis of Dy2TiO5 Single-Phase Crystalline Nanopowders and Investigation of Their Properties. Inorganic Materials: Applied Research, 2018, 9, 291-296.	0.5	4
79	Metal-Doped MgB2 by Thermal Explosion: A TRXRD Study. International Journal of Self-Propagating High-Temperature Synthesis, 2018, 27, 18-25.	0.5	3
80	Combustion synthesis of high-temperature ZrB2-SiC ceramics. Journal of the European Ceramic Society, 2018, 38, 2792-2801.	5.7	26
81	Crystallization of amorphous Cu50Ti50 alloy prepared by high-energy ball milling. Journal of Alloys and Compounds, 2018, 741, 575-579.	5.5	32
82	Crystallization of a Mechanically Activated CuTi Alloy. Doklady Physics, 2018, 63, 45-49.	0.7	2
83	Self-sustained exothermal waves in amorphous and nanocrystalline films: A comparative study. Journal of Alloys and Compounds, 2018, 749, 44-51.	5.5	10
84	Self-propagating high-temperature synthesis of nanocomposite ceramics TaSi2-SiC with hierarchical structure and superior properties. Journal of the European Ceramic Society, 2018, 38, 433-443.	5.7	36
85	Conductive TiB2–AlN–BN-Based Composite SHS Ceramics. Russian Journal of Non-Ferrous Metals, 2018, 59, 658-663.	0.6	2
86	Determination of the Thermal Expansion Coefficient of Boron Carbide Đ'13Đ¡2. High Temperature, 2018, 56, 668-672.	1.0	9
87	Density Functional Calculations for Disordered Boron Carbide Crystals. Russian Journal of Physical Chemistry A, 2018, 92, 2341-2344.	0.6	1
88	Transformations of Iron (III) Precursors in a Wave of Flameless RDX Combustion. International Journal of Self-Propagating High-Temperature Synthesis, 2018, 27, 162-166.	0.5	6
89	Formation of Acquired Grain-Growth Inhibitor in the Production of Anisotropic Electrical Steel. Steel in Translation, 2018, 48, 541-546.	0.3	1
90	Electrically Conducting Ceramics Based on Al–AlN–TiB2. High Temperature, 2018, 56, 527-531.	1.0	1

#	Article	IF	CITATIONS
91	Synthesis of Zirconium Diboride Nanoparticles by the Reaction of ZrCl4 with NaBH4 in an Ionic Potassium Bromide Melt. Russian Journal of General Chemistry, 2018, 88, 1757-1758.	0.8	3
92	Crystallization of Amorphous Antimony at Room Temperature: Non-Uniqueness of Patterning Route. International Journal of Self-Propagating High-Temperature Synthesis, 2018, 27, 180-183.	0.5	2
93	Synthesis of the Ti2AlC MAX Phase with a Reduction Step via Combustion of a TiO2 + Mg + Al + C Mixture. Inorganic Materials, 2018, 54, 949-952.	0.8	8
94	Features of Production and High-Temperature Oxidation of SHS Ceramics Based on Zirconium Boride and Zirconium Silicide. Russian Journal of Non-Ferrous Metals, 2018, 59, 311-322.	0.6	3
95	Composition and Structure of (Zr0.37Ti0.63)3AlC2 MAX Phase Crystals Prepared by Self-Propagating High-Temperature Synthesis. Inorganic Materials, 2018, 54, 953-956.	0.8	2
96	Solution combustion synthesis of nano-catalysts with a hierarchical structure. Journal of Catalysis, 2018, 364, 112-124.	6.2	29
97	Synthesis of a new MAX phase in the Ti–Zr–Al–C system. Mendeleev Communications, 2017, 27, 59-60.	1.6	7
98	New Insight into the Formation of Hybrid Perovskite Nanowires via Structure Directing Adducts. Chemistry of Materials, 2017, 29, 587-594.	6.7	68
99	Oxynitrides by aluminothermic SHS in nitrogen gas: Influence of nitrogen pressure. International Journal of Self-Propagating High-Temperature Synthesis, 2017, 26, 71-74.	0.5	1
100	Combustion synthesis in the Ni–Al–Nb ternary system: A Time-Resolved X-ray Diffraction study. Results in Physics, 2017, 7, 1878-1882.	4.1	5
101	Reaction synthesis of the Ti2AlN MAX-phase. Russian Journal of Non-Ferrous Metals, 2017, 58, 303-307.	0.6	14
102	Dynamics of phase formation during the synthesis of magnesium diboride from elements in thermal explosion mode. Russian Journal of Non-Ferrous Metals, 2017, 58, 396-404.	0.6	3
103	Ignition and phase formation in the Zr–Al–C system. Combustion, Explosion and Shock Waves, 2017, 53, 171-175.	0.8	5
104	Time-resolved X-ray diffraction study of the transition of an amorphous TiCu alloy to the crystalline state. Doklady Physics, 2017, 62, 111-114.	0.7	6
105	The features of combustion synthesis of aluminum and carbon doped magnesium diboride. Physica C: Superconductivity and Its Applications, 2017, 541, 1-9.	1.2	5
106	X-ray diffraction study of self-propagating high-temperature synthesis in the Zr–Al–C system. Russian Journal of Inorganic Chemistry, 2017, 62, 1638-1644.	1.3	7
107	FEATURES OF PRODUCTION AND HIGH-TEMPERATURE OXIDATION OF SHS-CERAMICS BASED ON ZIRCONIUM BORIDE AND ZIRCONIUM SILICIDE. Izvestiya Vuzov Poroshkovaya Metallurgiya I Funktsional'nye Pokrytiya, 2017, , 29-41.	0.2	4
108	PHASE FORMATION IN TI–AL–C SYSTEM DURING SHS. Izvestiya Vuzov Poroshkovaya Metallurgiya I Funktsional'nye Pokrytiya, 2017, , 11-18.	0.2	2

#	Article	IF	CITATIONS
109	Time-Resolved X-Ray and Synchrotron-Ray Diffraction. , 2017, , 388-391.		0
110	Influence of the synthesis conditions of boron carbide on its structural parameters. Russian Journal of Non-Ferrous Metals, 2016, 57, 604-609.	0.6	0
111	Combustion of Ti–Al–C compacts in air and helium: A TRXRD study. International Journal of Self-Propagating High-Temperature Synthesis, 2016, 25, 30-34.	O.5	17
112	Preparation of Ti2AlN by reactive sintering. International Journal of Self-Propagating High-Temperature Synthesis, 2016, 25, 35-38.	0.5	6
113	The kinetics and mechanism of combusted Zr–B–Si mixtures and the structural features of ceramics based on zirconium boride and silicide. Ceramics International, 2016, 42, 16758-16765.	4.8	18
114	SHS in the Zr–Al–C system: A time-resolved XRD study. International Journal of Self-Propagating High-Temperature Synthesis, 2016, 25, 149-154.	0.5	3
115	Phase formation dynamics upon thermal explosion synthesis of magnesium diboride. Ceramics International, 2016, 42, 2951-2959.	4.8	14
116	Exothermic Self-Sustained Waves with Amorphous Nickel. Journal of Physical Chemistry C, 2016, 120, 5827-5838.	3.1	23
117	Structural features and magnetic behavior of nanocrystalline powders of terbium oxide prepared by the thermal decomposition of terbium acetate in air. Journal of Alloys and Compounds, 2016, 657, 163-173.	5.5	13
118	Magnesiothermic SHS of boron carbide in conditions of temperature gradients. International Journal of Self-Propagating High-Temperature Synthesis, 2015, 24, 216-219.	0.5	3
119	Experimental investigation of electrical and optical phenomena during combustion of two-layer energetic condensed (Zr + CuO + LiF)–(Zr + BaCrO4 + LiF) systems. Inorganic Materials: Applied Research, 2015, 6, 542-546.	0.5	1
120	The features of combustion and structure formation of ceramic materials in the TiC–Ti3POx–CaO system. Ceramics International, 2015, 41, 8177-8185.	4.8	16
121	Self-propagating high-temperature synthesis in the Ti-Si-C system: Features of product patterning. Nanotechnologies in Russia, 2015, 10, 67-74.	0.7	19
122	Production of ultra-high temperature carbide (Ta,Zr)C by self-propagating high-temperature synthesis of mechanically activated mixtures. Ceramics International, 2015, 41, 8885-8893.	4.8	39
123	SHS of boron carbide: Influence of combustion temperature. International Journal of Self-Propagating High-Temperature Synthesis, 2015, 24, 33-37.	0.5	5
124	Influence of synthesis conditions on the structure and phase formation during the SHS hydration of titanium. Russian Journal of Non-Ferrous Metals, 2015, 56, 86-91.	0.6	1
125	Silicon carbide ceramics SHS-produced from mechanoactivated Si–C–B mixtures. International Journal of Self-Propagating High-Temperature Synthesis, 2015, 24, 119-127.	0.5	14
126	Flameless Combustion Synthesis of Ni and Ag Nanoparticles in Ballasted Systems: A Timeâ€Resolved Xâ€ray Diffraction Study. Propellants, Explosives, Pyrotechnics, 2015, 40, 88-94.	1.6	9

#	Article	IF	CITATIONS
127	SHS of MAX compounds in the Ti-Si-C system: Influence of mechanical activation. International Journal of Self-Propagating High-Temperature Synthesis, 2014, 23, 141-144.	0.5	11
128	Formation of nanolaminate structures in the Ti-Si-C system: A crystallochemical study. International Journal of Self-Propagating High-Temperature Synthesis, 2014, 23, 217-221.	0.5	20
129	SHS hydrogenation of group IV metals as studied by time-resolved XRD. International Journal of Self-Propagating High-Temperature Synthesis, 2014, 23, 198-202.	0.5	3
130	Formation of nanosized particles of nickel and silver in a wave of flameless combustion of cellulose nitrate in ballasted systems. Doklady Physical Chemistry, 2014, 458, 133-137.	0.9	3
131	Mechanical activation of a hard magnetic Fe-Cr-Co alloy powder charge. Russian Metallurgy (Metally), 2014, 255-560.	0.5	3
132	In Situ Preparation of Highly Stable Ni-Based Supported Catalysts by Solution Combustion Synthesis. Journal of Physical Chemistry C, 2014, 118, 26191-26198.	3.1	58
133	The features of combustion and structure formation of ceramic materials in the Cr–Al–Si–B system. Ceramics International, 2014, 40, 16299-16308.	4.8	10
134	SHS in the Ni-Al system: A TRXRD study of product patterning. International Journal of Self-Propagating High-Temperature Synthesis, 2014, 23, 101-105.	0.5	6
135	Self-propagating high-temperature synthesis of advanced ceramics in the Mo–Si–B system: Kinetics and mechanism of combustion and structure formation. Ceramics International, 2014, 40, 6541-6552.	4.8	51
136	2-dimensional GEM detector with FEE based on the nXYTER ASIC. Journal of Instrumentation, 2014, 9, C09026-C09026.	1.2	1
137	SHS hydrogenation of titanium: Some structural and kinetic features. International Journal of Self-Propagating High-Temperature Synthesis, 2013, 22, 114-118.	0.5	8
138	Deposition of Ni-Al coatings onto copper by mechanical/heat treatment. International Journal of Self-Propagating High-Temperature Synthesis, 2013, 22, 103-109.	0.5	3
139	Combustion synthesis in the Ni-Al-W system: Some structural features. International Journal of Self-Propagating High-Temperature Synthesis, 2013, 22, 110-113.	0.5	4
140	Behavior of the Ti-Al system during mechanical activation. International Journal of Self-Propagating High-Temperature Synthesis, 2013, 22, 56-59.	0.5	7
141	Solution combustion synthesis: Dynamics of phase formation for highly porous nickel. Doklady Physical Chemistry, 2013, 449, 48-51.	0.9	11
142	Influence of the high energy ball milling on structure and reactivity of the Ni+Al powder mixture. Journal of Alloys and Compounds, 2013, 577, 600-605.	5.5	75
143	SHS of TiC-TiNi composites: Effect of initial temperature and nanosized refractory additives. International Journal of Self-Propagating High-Temperature Synthesis, 2012, 21, 202-211.	0.5	6
144	SHS of graded Ti-Al-C ceramics: Composition of transition layers. International Journal of Self-Propagating High-Temperature Synthesis, 2012, 21, 231-235.	0.5	3

#	Article	IF	CITATIONS
145	Regular features of combustion of CaO2/Al/Ti/Cr/B hybrid mixtures. Combustion, Explosion and Shock Waves, 2011, 47, 671-676.	0.8	8
146	Cast silicides of molybdenum, tungsten, and niobium by combustion synthesis. International Journal of Self-Propagating High-Temperature Synthesis, 2011, 20, 100-106.	0.5	6
147	Effect of mechanical activation on thermal explosion in Ni-Al mixtures. International Journal of Self-Propagating High-Temperature Synthesis, 2010, 19, 120-125.	0.5	27
148	Deposition of composite metallic coating onto Al through mechanical impregnation followed by thermal treatment. International Journal of Self-Propagating High-Temperature Synthesis, 2010, 19, 178-185.	0.5	0
149	Thermal decomposition of TiH2: A TRXRD study. International Journal of Self-Propagating High-Temperature Synthesis, 2010, 19, 253-257.	0.5	16
150	Criteria of the Critical State of the Ni—Al System during Mechanical Activation. Combustion, Explosion and Shock Waves, 2010, 46, 457-463.	0.8	14
151	Dynamics of phase transformation during thermal explosion in the Al–Ni system: Influence of mechanical activation. Physica B: Condensed Matter, 2010, 405, 778-784.	2.7	91
152	Effect of heat release conditions on the phase composition of the combustion products of a Fe2O3/TiO2/Al/C thermite mixture. Combustion, Explosion and Shock Waves, 2008, 44, 405-409.	0.8	3
153	Dynamics of phase formation during combustion of Zr and Hf in air. International Journal of Self-Propagating High-Temperature Synthesis, 2007, 16, 169-174.	0.5	7
154	Phase constitution of the combustion products of thermite mixtures modified by titanium oxide. Combustion, Explosion and Shock Waves, 2007, 43, 674-681.	0.8	3
155	On the mechanism of heterogeneous reaction and phase formation in Ti/Al multilayer nanofilms. Acta Materialia, 2005, 53, 1225-1231.	7.9	114
156	Combustion of a Fe2O3-TiO2-Al-C Powder Mixture in the SHS Regime and the Structure of the Combustion Products. Combustion, Explosion and Shock Waves, 2005, 41, 414-420.	0.8	6
157	Equilibrium of Products of Self-Propagating High-Temperature Synthesis. Doklady Physical Chemistry, 2004, 394, 34-38.	0.9	16
158	Title is missing!. Combustion, Explosion and Shock Waves, 2001, 37, 673-677.	0.8	2
159	Autowave Propagation of Exothermic Reactions in Ti–Al Thin Multilayer Films. Doklady Physical Chemistry, 2001, 381, 283-287.	0.9	13
160	The mechanism of formation of copper aluminide in the thermal explosion mode. Russian Chemical Bulletin, 2000, 49, 1954-1959.	1.5	3
161	Anomalous Hall effect in granular Fe/SiO2 films in the tunneling-conduction regime. JETP Letters, 1999, 70, 90-96.	1.4	51